Supporting Information

Luminescent silicon nanocrystals appended with photoswitchable azobenzene units.

Marco Villa, Sara Angeloni, Alberto Bianco, Alessandro Gradone, Vittorio Morandi, Paola Ceroni

Sommario

1. Materials and methods

All reagents were purchased from Sigma-Aldrich and used without further purification, unless otherwise stated. Dry toluene was obtained via distillation over calcium chloride under nitrogen atmosphere.

Nuclear magnetic resonance spectra ^{1}H (400.72 MHz) and ^{13}C (100.77 MHz) were recorded on an ARX Varian INOVA 400 (400MHz) spectrometer, signals of the residual protic solvent $CHCl_3$ at 7.26 ppm and DMSO-d_6 at 2.50 ppm were used as internal references, instead of TMS. As for ^{13}C NMR spectra, the central resonance of the triplet for $CDCl_3$ at 77.16 ppm was used as internal references.[1] The resonance multiplicities in the ^{1}H NMR spectra are described as "s" (singlet), "d"(doublet), "t" (triplet), "q" (quartet), "quint" (quintet) "sept" (septet) "m" (multiplet) or "b" (broad).

2. Synthetic procedures

2.1. Synthesis of chlorosilane-passivated SiNCs (Si-DMVSiCl)

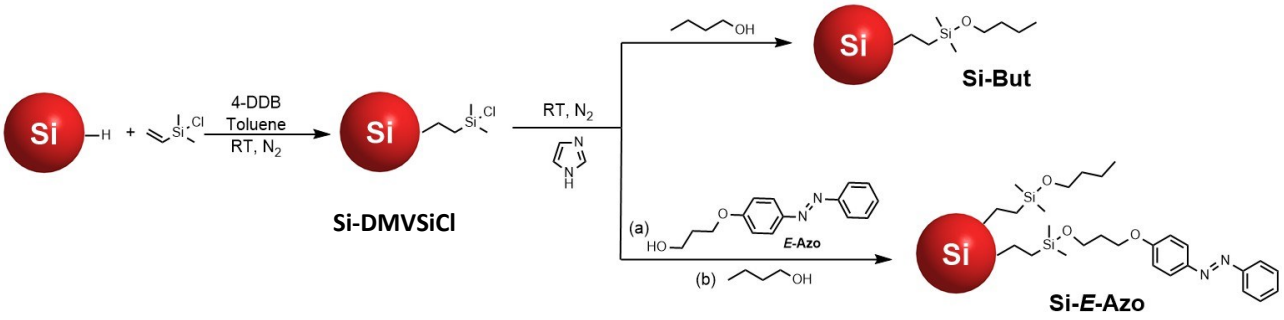

Scheme 1. *Synthetic procedure for the functionalization of hydride-terminated SiNCs by azobenzene*

Hydride-terminated silicon nanocrystals (H-SiNCs) were prepared by disproportionation of hydrogen silsesquioxane (HSQ, $[HSiO_{3/2}]_n$) at 1100°C. The so-obtained SiNCs embedded in SiO_2 matrix were liberated by the etching procedure using a mixture of EtOH:H_2O:HF=1:1:1. The complete procedure is described in the literature.[2,3] H-SiNCs, obtained after the etching procedure of 300 mg oxide-embedded SiNCs powder, were dispersed in 1.5 mL of dry toluene and two milligrams of 4-decylbenzene diazonium tetrafluoroborate (4-DDB, about 6 µmol) were added together with 400 µL of chloro(dimethyl)vinylsilane (3 mmol) to obtain the chlorosilane-passivated SiNCs (**Si-DMVSiCl** in Scheme 1). The mixture was stirred overnight inside a nitrogen-filled glovebox at RT. The mixture of chlorosilane-passivated SiNCs was then filtered, concentrated under vacuum to remove the excess of chloro(dimethyl)vinylsilane, then re-dispersed in 3 mL of dry toluene and stored under inert atmosphere.

2.2. Synthesis of (E)-3-(4-(phenyldiazenyl) phenoxy) propan-1-ol (*E*-AZO)[4]

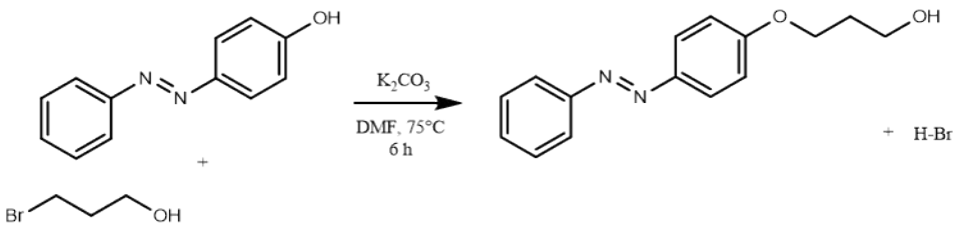

To a suspension of degassed dimethylformamide (DMF, 10 mL) and dry K_2CO_3 (525 mg, 3.8 mmol), under nitrogen atmosphere, 4-phenylazophenol (507 mg, 2.56 mmol), was added at room temperature. The

resulting mixture was stirred until the complete dissolution of the solid compounds. Then, 3-bromo-1-propanol (0.3 mL, 3.3 mmol) was added. The reaction mixture was stirred for 6 hours at 75°C and then cooled down to room temperature. The formation of an orange precipitate was observed. 80 mL of distilled water were added to the reaction mixture, the organic phase was separated from the aqueous one and the latter was extracted 4 times using 20 mL of DCM each time. The combined organic phases were dried over anhydrous Na_2SO_4, filtered and concentrated *in vacuo*. The crude orange oil was purified via flash chromatography using DCM/EtOAc 8:1 as the eluent. The product ***E*-Azo** was recovered as an orange solid after evaporation of solvents, with a yield of 88% (577 mg, 2.25 mmol).

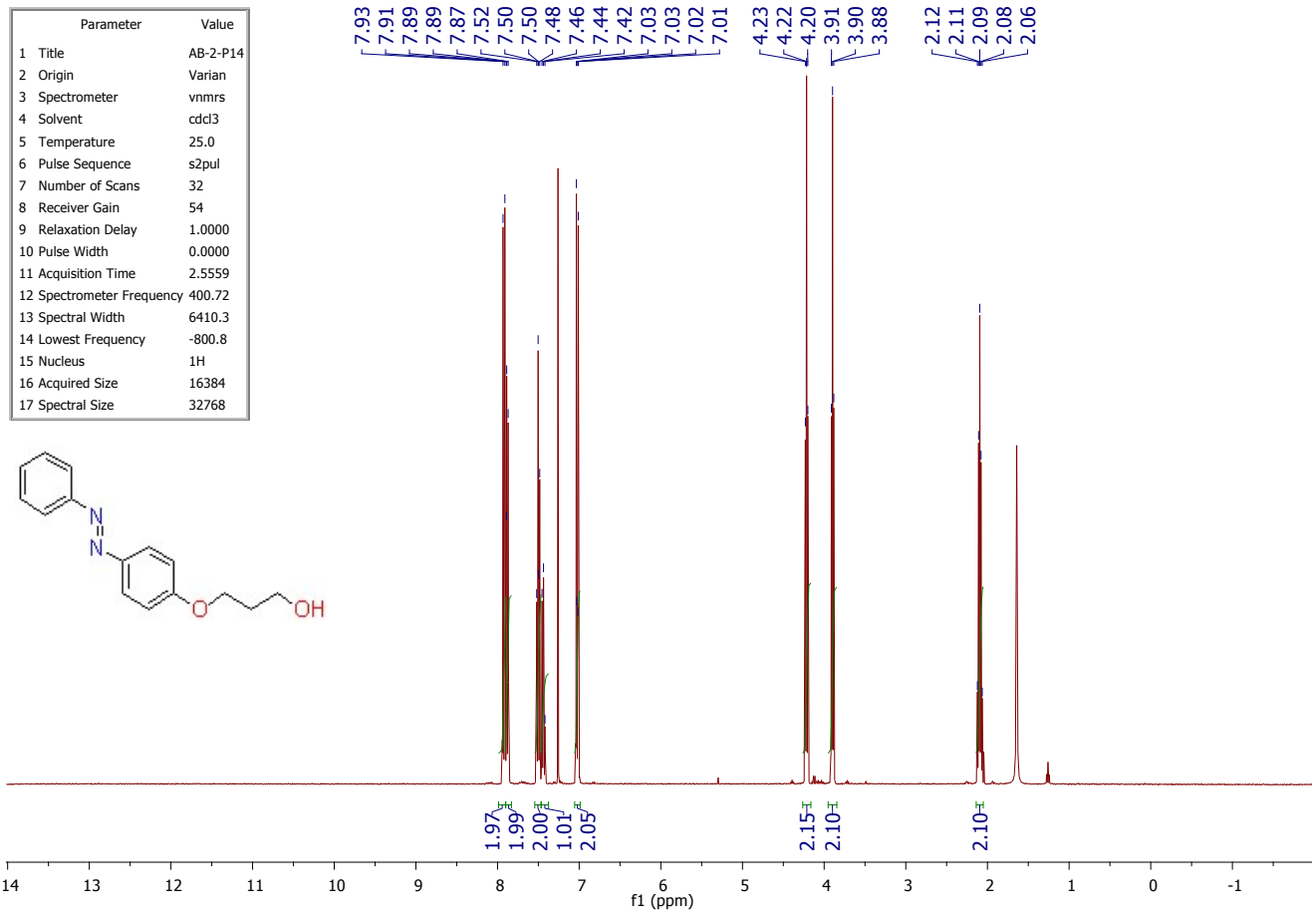

Figure S1. *^{1}H-NMR spectrum of **E-AZO** ($CDCl_3$, 400.72 MHz)*

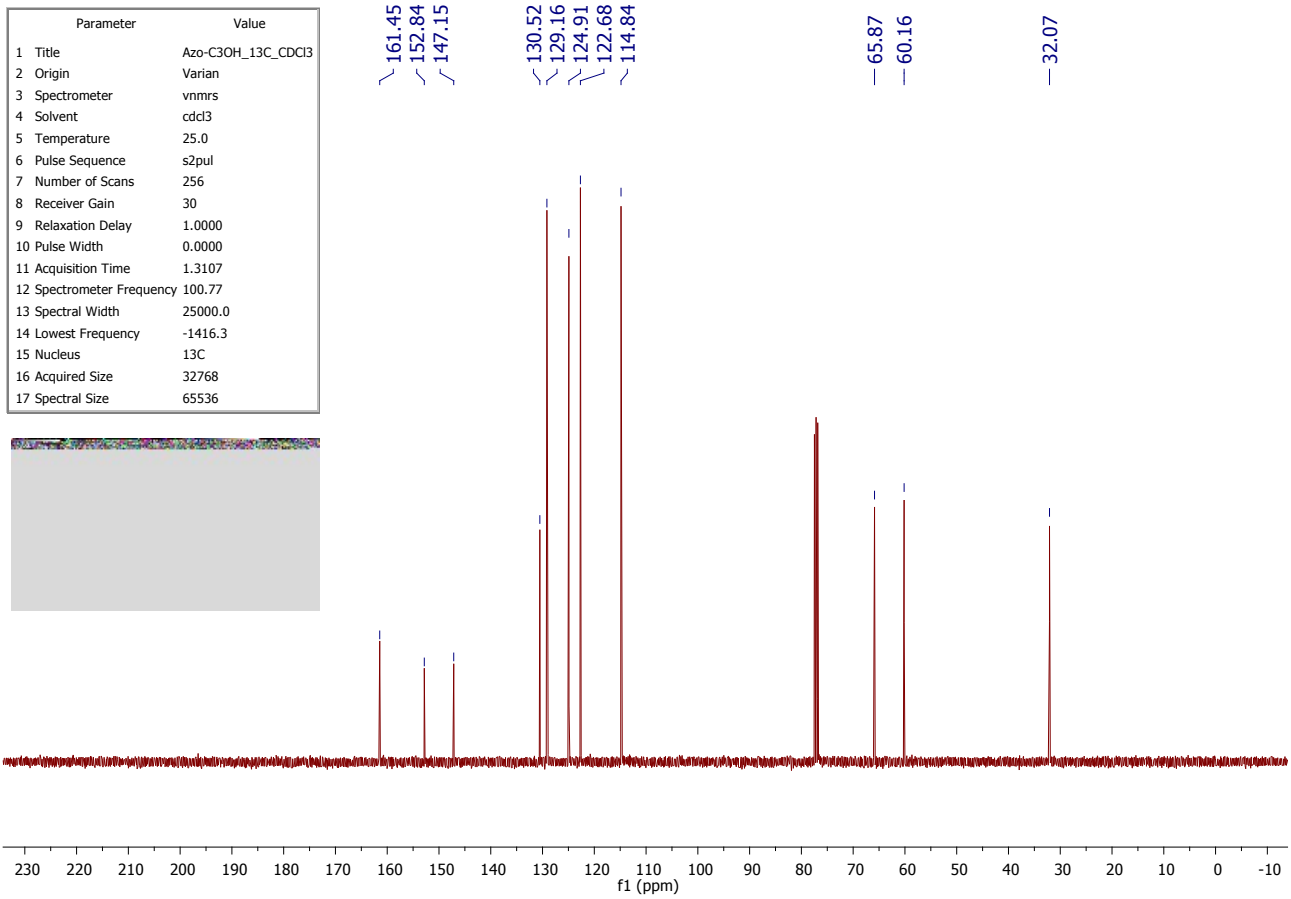

Figure S2. *^{13}C-NMR spectrum of **E-AZO** ($CDCl_3$, 100.77 MHz)*

^{1}H-NMR (400.72 MHz, $CDCl_3$, ppm), δ = 7.92(d, J = 9.0 Hz, 2H), 7.88(d, J = 7.1 Hz, 2H), 7.50 (t, J = 7.1 Hz, 2H), 7.42 ppm (t, J = 7.2 Hz, 1H), 7.02 (dt, J = 9.0 Hz, 2.6 Hz, 2H), 4.22 (t, J = 6.0 Hz, 2H), 3.90 ppm (t, J = 5.9 Hz, 2H), 2.09 (quint, J = 6.0 Hz, 2H).

^{13}C-NMR (100.77 MHz, $CDCl_3$, ppm), δ = 161.45, 152.84, 147.15, 130.52, 129.16, 124.91, 122.68, 114.84, 65.87, 60.16, 32.07.

2.3. SiNCs passivation with butanol (Si-But)

The **Si-But** reference sample (Scheme 1) was synthesised by adding butanol (0.14 mL, 1.5 mmol) to a 1 mL of the previously prepared chlorosilane-passivated SiNCs, together with a catalytic amount of imidazole. The reaction was stirred for 12 h inside a nitrogen-filled glove box. 5 mL of dry ACN were added to the reaction mixture, the precipitated SiNCs were collected on a PTFE filter, washed 3 times with 5 mL of dry ACN and then dispersed in 1 mL of distilled toluene.

2.4. Passivation of SiNCs with (E)-3-(4- (phenyldiazenyl) phenoxy) propan-1-ol (Si-*E*-Azo)

Si-*E*-Azo sample (Scheme 1) was synthesised by adding (E)-3-(4- (phenyldiazenyl) phenoxy) propan-1-ol (33 mg, 0.13 mmol) to a 1 mL of the previously prepared chlorosilane-passivated SiNCs solution, together with a catalytic amount of imidazole. The reaction was stirred for 12 h inside a nitrogen-filled glove box and then 0.1 mL of butanol was added in order to cap the non-reacted chlorosilane groups on the nanocrystals. The reaction mixture was stirred for an additional hour. Then, the sample was washed by adding 5 mL of dry ACN to the reaction mixture, the precipitated SiNCs were collected on a PTFE filter, washed 3 times with 5 mL of dry ACN and then dispersed in 1 mL of distilled toluene or cyclohexane.

3. Dynamic light scattering

The determination of the hydrodynamic diameter distributions of the nanocrystals was carried out by DLS measurements with a Malvern Nano ZS instrument with a 633 nm laser diode (Figure S3). The samples were housed in quartz cuvettes of 1 cm optical path length. The size distribution of **Si-*E*-Azo** (a) and **Si-*Z*-Azo** (b) in toluene yields an average hydrodynamic diameter of 10 nm with a low polydispersity index (PdI = 0.13) and an average hydrodynamic diameter of 8 nm with PdI = 0.14 for **Si-But** (c).

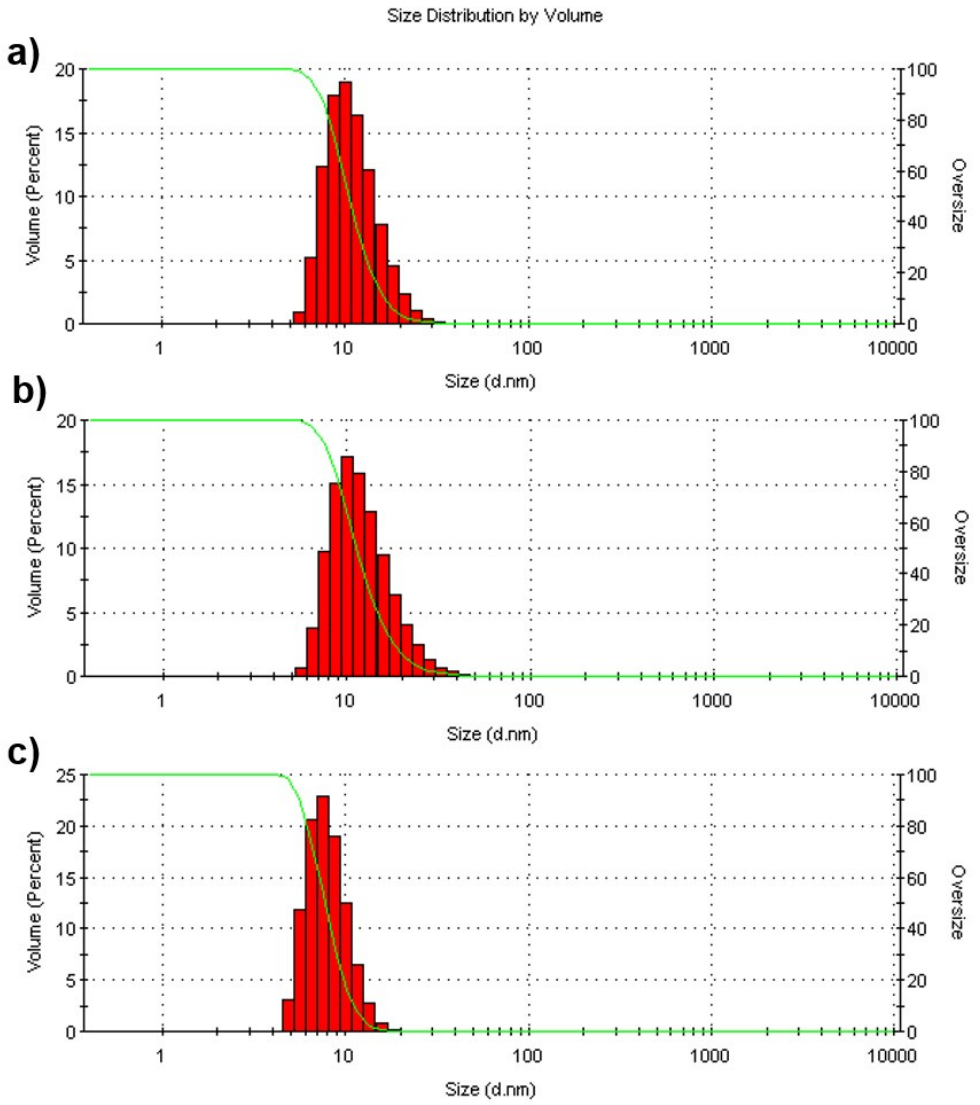

Figure S3. *Dynamic light scattering analysis of 1.00 x 10^{-6} M **Si-E-Azo** (a), **Si-Z-Azo** (b) and **Si-But** in toluene.*

4. Photophysical and photochemical measurements in solution

Photophysical measurements were carried out in distilled dry toluene at 298 K or at 293 K or at 279 K. UV-visible absorption spectra were recorded with a Varian Cary 50 BIO spectrophotometer, using quartz cuvettes with 1.0 cm path length. Emission spectra were obtained with either a Perkin Elmer LS55 spectrofluorometer, equipped with a Hamamatsu R928 phototube, or an Edinburgh FLS920 spectrofluorometer equipped with a Ge-detector for emission in the NIR spectral region. Correction of the emission spectra for detector sensitivity in the 550-1000 nm spectral region was performed by a calibrated lamp.[5] Excitation spectra in the visible range were acquired with the fluorimeter Perkin-

Elmer LS55. Emission quantum yields were measured following the method of Demas and Crosby[6] (standard used: $[Ru(bpy)_3]^{2+}$ in air-equilibrated aqueous solution $\Phi = 0.0405$[7] and HITCI (1,1',3,3,3',3'-hexamethyl-indotricarbocyanine iodide) in EtOH $\Phi = 0.30$).[8] Emission intensity decay measurements in the range 10 μs to 1 s were performed on a homemade time-resolved phosphorimeter.

Photochemical reactions were performed at room temperature on thoroughly stirred degassed solutions by using a Helios Italquartz Polymer 125 medium pressure Hg lamp (125 W).

The estimated experimental errors are: 2 nm on the absorption and emission band maximum, 5% on the molar absorption coefficient and luminescence lifetime, and 10% on the luminescence and photoisomerization quantum yields. The size of the nanocrystals was determined by comparing the energy of the PL band maximum with the size-band gap correlation curve by following the method reported in a previous work.[3]

The partition ratio of **Si-*E*-Azo** and **Si-*Z*-Azo** between cyclohexane and methanol was calculated by changes in the azobenzene π,π* absorption band at 350 nm in cyclohexane before and after mixing with methanol.

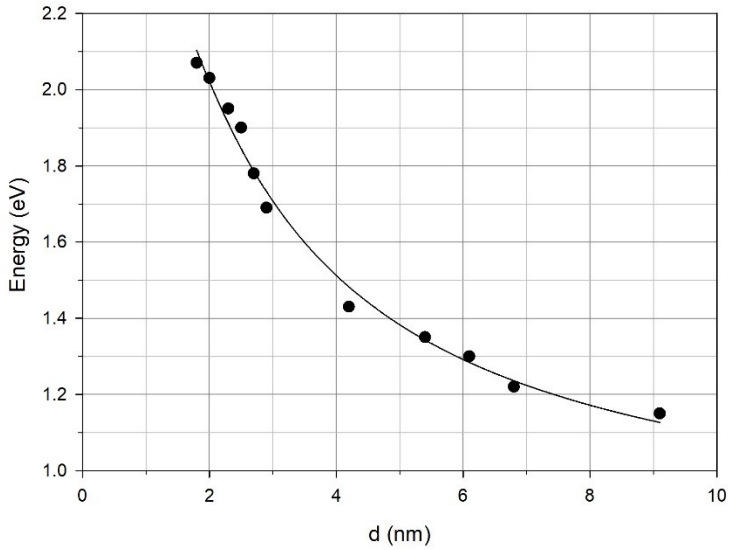

Figure S4. *PL peak energy vs. core diameter for alkyl passivated colloidal SiNCs; data from ref. 3.*

On the basis of the molar absorption coefficients of the reference ***E*-Azo** ($\varepsilon_{350\ nm}$ = 28000 M^{-1} cm^{-1}) and the one of the SiNCs ($\varepsilon_{400\ nm} = 5 \times 10^4$ M^{-1} cm^{-1} for 3 nm diameter),[9,10] we can estimate an average number of about 15 ***E*-Azo** per SiNC.

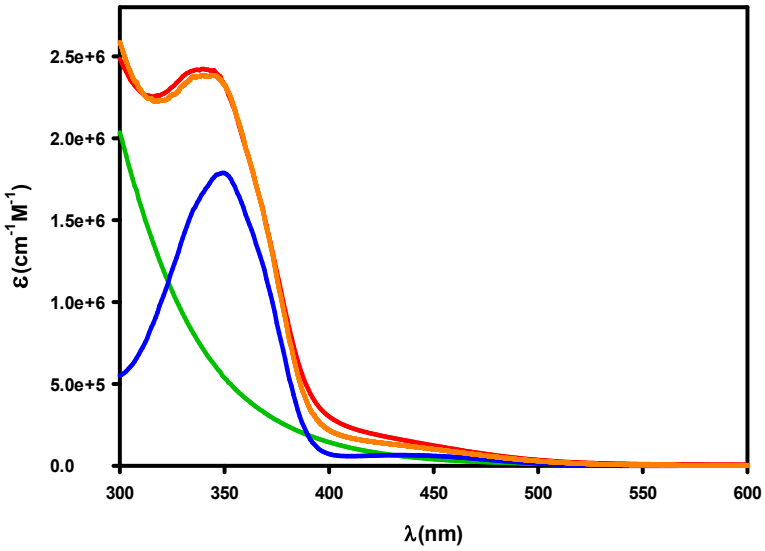

Figure S5. *Absorption spectra of* ***Si-But*** *(green line),* ***E-Azo*** *(blue line),* ***Si-E-Azo*** *(red line) and of a mixture of* ***Si-But*** *and* ***E-Azo*** *(orange line) in the molar ratio 1:15 in dry toluene****.*** *These spectra were used for the evaluation of the average number of* ***E-Azo*** *per SiNC.*

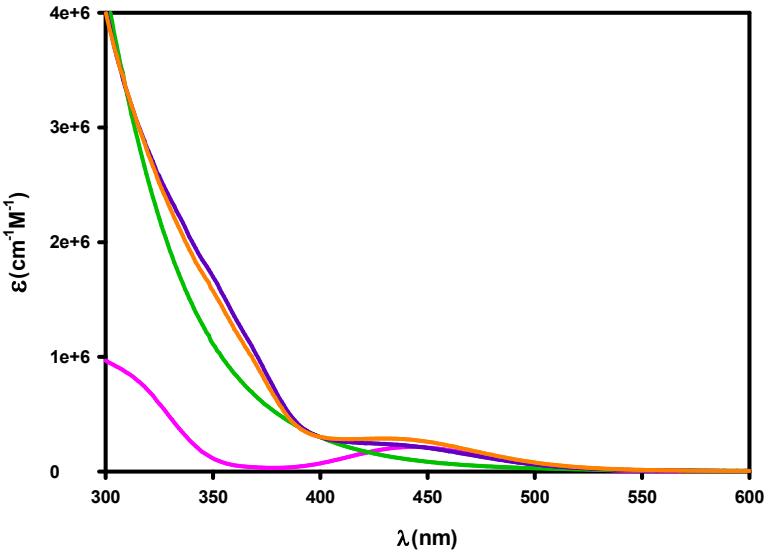

Figure S6. *Absorption spectra of* ***Si-But*** *(green line),* ***Z-Azo*** *(pink line),* ***Si-Z-Azo*** *(purple line) and of a mixture of* ***Si-But*** *and* ***Z-Azo*** *(orange line) in the molar ratio 1:15 in dry toluene. These spectra were used for the evaluation of the average number of* ***Z-Azo*** *per SiNC.*

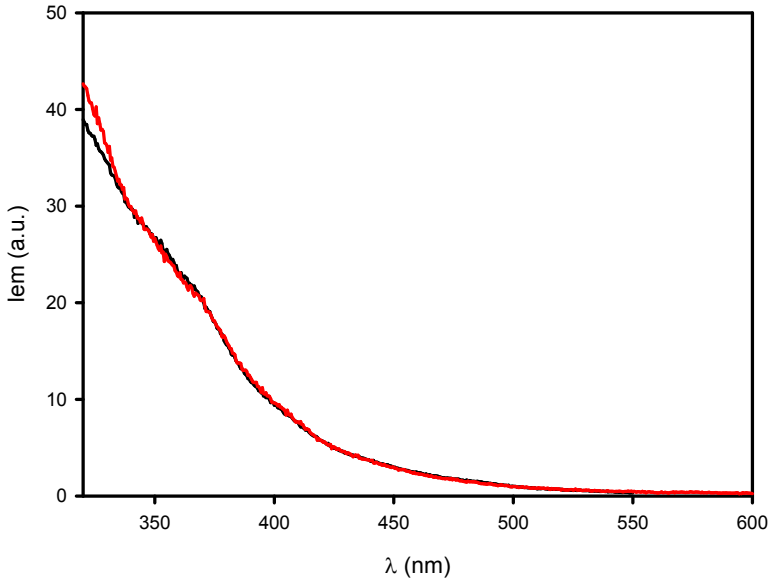

Figure S7. *Excitation spectra of* ***Si-E-Azo*** *(red line) and* ***Si-But*** *(black line) in toluene* (λ_{em} *= 730 nm).*

4.1. Photoisomerization Quantum Yields

We calculated the composition of the photostationary state obtained upon irradiation at 365 nm by ^{1}H-NMR spectroscopy (Figure S8).

^{1}H-NMR spectra of an **Azo** solution in DMSO-d_6 were acquired before and after prolonged irradiation at 365 nm to obtain the photostationary state. No evidence of ***E*-Azo** isomer is present in the ^{1}H-NMR spectrum reported in Figure S8 (green line), demonstrating that the composition of the 365-nm photostationary state is **Z-Azo** > 99%. Therefore, the molar absorption coefficient of the ***Z*-Azo** isomer was evaluated by the absorption spectrum of the 365-nm photostationary state (blue line in Figure 2a).

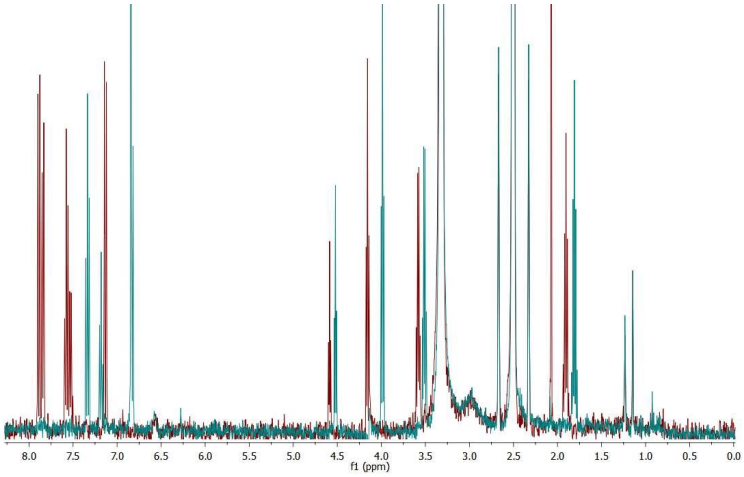

Figure S8. E-Azo *^{1}H NMR (red spectrum) compared to* ***Z-Azo*** *^{1}H NMR (green spectrum)*

***E*-Azo ^{1}H NMR (400.72 MHz, DMSO-d6)** δ 7.89 ppm (d, *J* = 8.9 Hz, 2H), 7.84 ppm (d, *J* = 7.6 Hz, 2H), 7.58 ppm (t, *J* = 7.4 Hz, 2H), 7.53 ppm (d, *J* = 6.9 Hz, 1H), 7.13 ppm (d, *J* = 8.9 Hz, 2H), 4.59 ppm (t, *J* =

5.2 Hz, 1H), 4.16 ppm (t, *J* = 6.4 Hz, 2H), 3.58 ppm (q, *J* = 5.9 Hz, 2H), 1.90 ppm (p, *J* = 6.4 Hz, 2H); 3.33 ppm (bs, H_2O), 2.67 ppm (s, DMSO), 2.50 ppm (s, DMSO), 2.33 ppm (s, DMSO), 2.09 ppm (s, Acetone), 1.24 ppm (bs, grease), 0.88-0.82 ppm (m, grease).

***Z*-Azo ^{1}H NMR (400.72 MHz, DMSO-d6)** δ 7.34 ppm (t, *J* = 7.8 Hz, 2H), 7.18 ppm (t, *J* = 7.4 Hz, 1H), 6.84 ppm (s, 5H), 6.82 ppm (s, 1H), 4.52 ppm (t, *J* = 5.2 Hz, 1H), 3.99 ppm (t, *J* = 6.3 Hz, 2H), 3.51 ppm (q, *J* = 6.0 Hz, 2H), 1.81 ppm (p, *J* = 6.2 Hz, 2H); 3.33 ppm (bs, H_2O), 2.67 ppm (s, DMSO), 2.50 ppm (s, DMSO), 2.33 ppm (s, DMSO), 2.09 ppm (s, Acetone), 1.24 ppm (bs, grease), 0.88-0.82 ppm (m, grease).

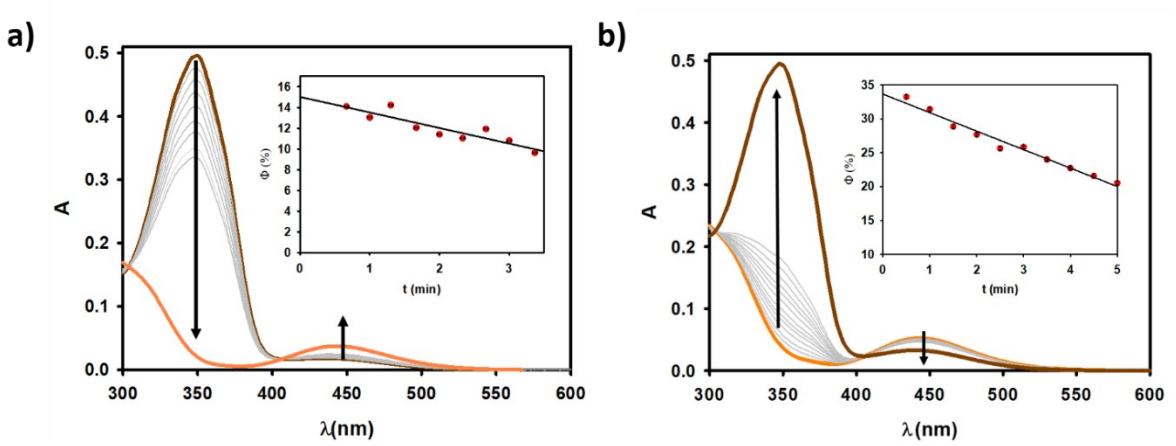

Figure S9. *Absorption spectra of an* ***Azo*** *solution in toluene a) before (dark orange spectrum), during (grey spectra) and after (light orange spectrum) irradiation at 365 nm, b) before (light orange spectrum), during (grey spectra) and after (dark orange spectrum) irradiation at 436 nm. Insets: photoisomerization QY with respect to the irradiation time.*

The photoisomerization quantum yields of azobenzene derivatives in toluene solutions were determined on the basis of the following molar absorption coefficients at 365 nm: ***E*-Azo** ε = 2.2×10^4 M^{-1} cm^{-1} , ε = 8×10^1 M^{-1} cm^{-1}, focusing our attention on two irradiating wavelength, 365 nm and 436 nm and using known solutions volumes (Figure S9). The $E \rightarrow Z$ photoisomerization quantum yield (λ_{irr}= 365 nm) was determined from the disappearance of the $\pi\pi^*$ absorption band of the azobenzene unit at 350 nm at low conversion percentages (extrapolation to t=0 was made). The fraction of light transmitted at the irradiation wavelength was considered in the calculation of the yields.

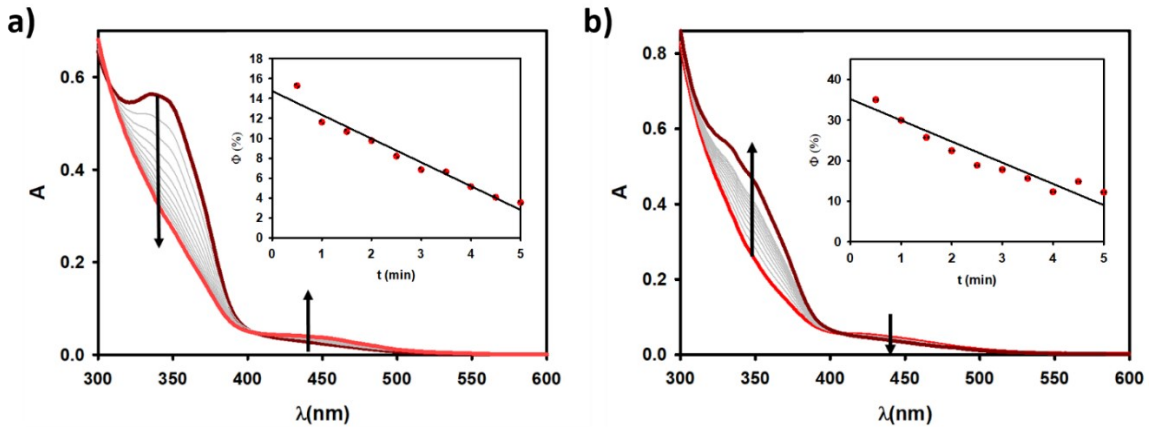

Figure S10. *Absorption spectra of a* ***Si-Azo*** *solution in toluene a) before (dark red spectrum), during (grey spectra) and after (light red spectrum) irradiation at 365 nm; b) before (light red spectrum), during (grey*

spectra) and after (dark red spectrum) irradiation at 436 nm. Insets: photoisomerization QY with respect to the irradiation time.

The photoisomerization QYs of **Si-Azo** (Figure S10) were measured in the same way, as for **Azo**. Considering the fraction of the light absorbed by the SiNCs in **Si-Azo** and correcting the total absorbed photons moles for this value, we can obtain the real amount of light absorbed by the azobenzene derivatives. The photoisomerization QY values are really close to the ones of the azobenzene model compound.

4.2. Thermal *Z*→*E* isomerization

Thermal *Z*→*E* isomerization was carried out by keeping the **Si-*Z*-Azo** and ***Z*-Azo** samples in the dark at 293K, until the **Si-*E*-Azo** and ***E*-Azo** were fully recovered. The kinetic constants (Figure 4a), k, were measured by acquiring absorption spectra each 5 minutes, for a total of ca. 3 hours, plotting the following equation:

$$ln(A_\infty - A_t) = ln(\varepsilon_E - \varepsilon_Z) + ln[Z]_0 - kt$$

where A_∞ is the fully recovered sample absorbance at 350 nm, A_t is the sample absorbance at 350 nm at "*t*" time, ε_E is the *E* isomer molar absorption coefficient at 350 nm, ε_Z is the *Z* isomer molar absorption coefficient at 350 nm, $[Z]_0$ is the *Z* isomer molar concentration at the zero time and t is the measurement time.

The same experiment was carried out in chloroform (Figure S11), a more polar solvent compared to toluene. The thermal *Z*→*E* isomerization is 15 times faster for the ***Z*-Azo** sample (k = 4 x 10^{-5} s^{-1}), as expected based on the literature reports.[11–13] In the case of **Si-*Z*-Azo** the thermal back isomerization to **Si-*E*-Azo** is still not linear as in toluene (Figure 4a); the rate of the thermal isomerization is comparable to the one of ***Z*-Azo** only in the final part of the experiment.

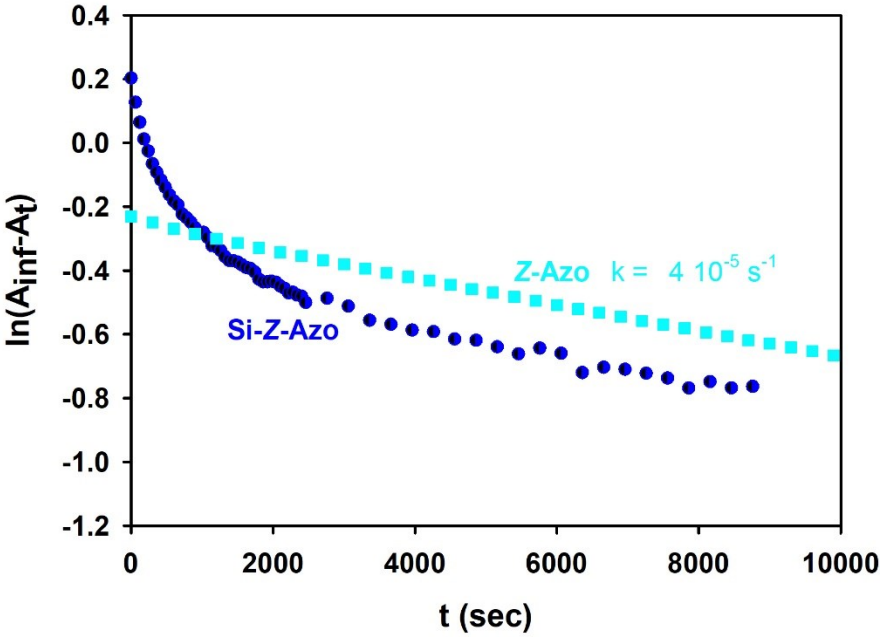

Figure S11. *Thermal isomerisation of* ***Z-Azo*** *(5.0x10^{-5} M, cyan squares) and* ***Si-Z-Azo*** *(2.5x10^{-6} M, blue circles) in chloroform solution at 293 K.*

4.3. Sensitization process measurements

Two identical solutions of **Si-*Z*-Azo** in dry toluene were prepared: one of them was kept in the dark at 261 K, while the second sample was irradiated at 660 nm and 261 K. Absorption spectra were acquired every 5 minutes for a total of 100 minutes for both the samples and the absorption values at 350 nm were plotted respect to the measurement time (Figure 4b).

The same experiment was also carried out at 279 K (Figure S12), but at this temperature the sensitization effect is less evident since the thermal isomerization is faster.

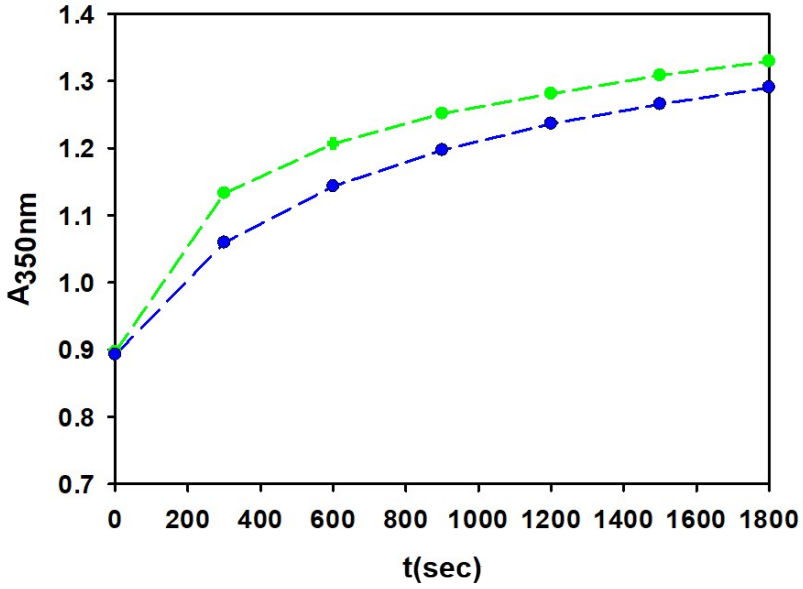

Figure S12. *Thermal (blue circles) vs photosensitised (green circles, λ_{irr} = 660 nm) isomerization of* ***Si-Z-Azo*** *in toluene at 279 K.*

5. Lifetime measurements

Figure S13 shows the luminescence intensity decay of **Si-But**, **Si-*E*-Azo** and **Si-*Z*-Azo** in toluene. The corresponding average lifetime values are reported in Table 1.

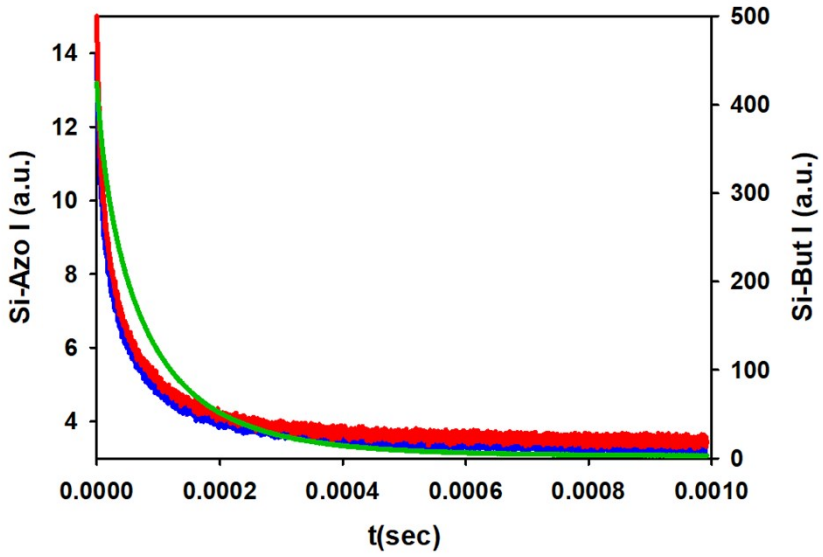

Figure S13. *Luminescence intensity decay of* ***Si-But*** *(green line, right y-axis),* ***Si-E-Azo*** *(red line, left y-axis) and* ***Si-Z-Azo*** *(blue line, left y-axis) toluene solutions.*

6. Morphological characterization and size distribution

Scanning transmission electron microscopy (STEM) high angle annular dark field (HAADF) characterization was carried out to estimate the morphology and the size distribution of the nanocrystal silicon core. A FEI Tecnai F20 instrument, equipped with a Schottky emitter and operated at 200 keV, was used. Silicon nanocrystals dispersed in chloroform were deposited on an Au grid with a lacey type – ultrathin continuous carbon film.

Figure S14 reports the STEM-HAADF images at different magnification of the silicon nanocrystals. The white spheres are relative to the Z contrast given by silicon nanocrystal core. The size distribution of the nanoparticles and their morphology are quite homogeneous, with some areas where two or more particles are superimposed (probably due to the drop casting step during the specimen preparation).

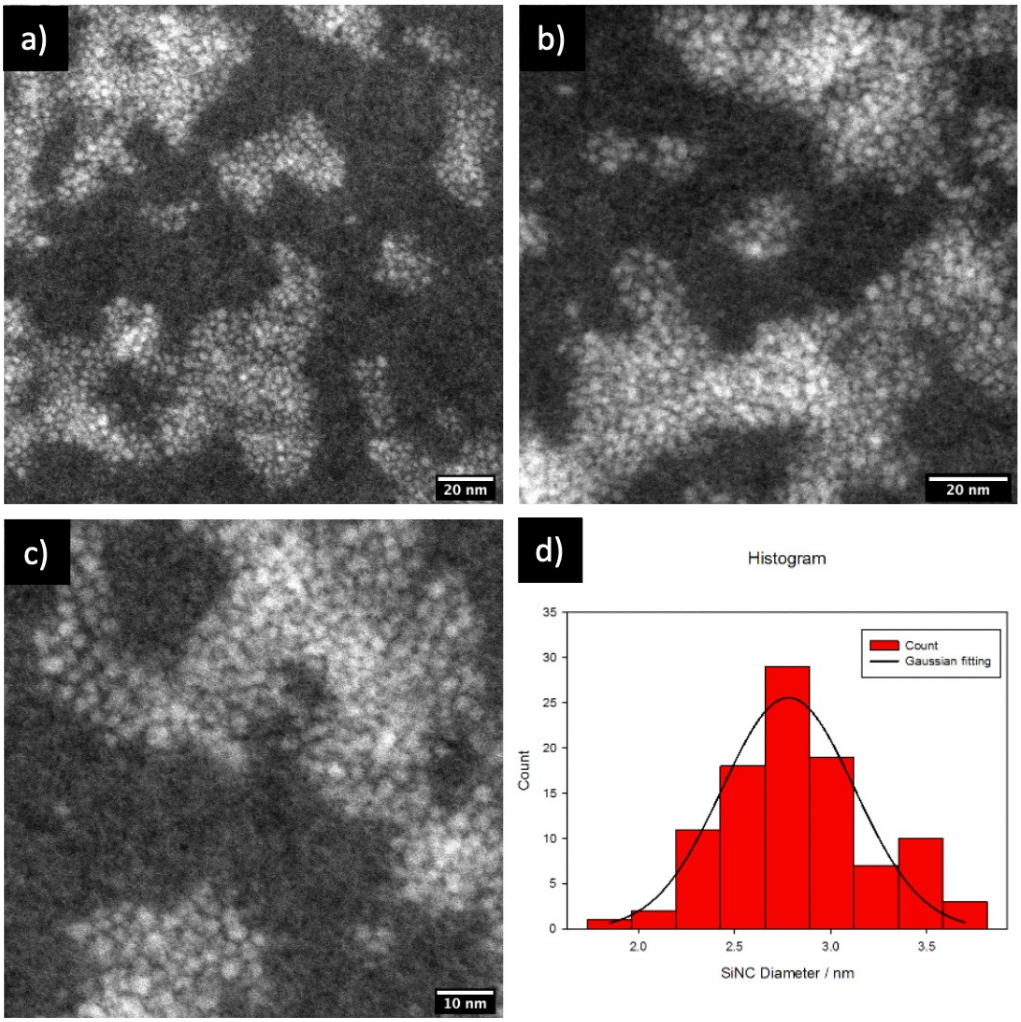

Figure S14. *a, b, c) STEM-HAADF images at different magnification of the* ***Si-Azo*** *nanoparticles. d) diameter size distribution of 100* ***Si-Azo*** *nanoparticles (red histogram), with its relative Gaussian fitting (black line) .*

The evaluation of the average diameter was made by analysis of several high magnification images (Figure S14d). 100 nanoparticles have been evaluated, considering the ones with spherical morphology. The fitting was made using the following Gaussian equation:

$$y = a\, e^{-0.5[(x - x_0)/b]^2}$$

The analysis gives an average diameter value of 2.8 nm with a standard deviation of 0.4 nm, well matching the size estimated by the optical properties (see above, Figure S4).

References

1 G. R. Fulmer, A. J. M. Miller, N. H. Sherden, H. E. Gottlieb, A. Nudelman, B. M. Stoltz, J. E. Bercaw and K. I. Goldberg, *Organometallics*, 2010, **29**, 2176–2179.

2 F. Romano, S. Angeloni, G. Morselli, R. Mazzaro, V. Morandi, J. R. Shell, X. Cao, B. W. Pogue and P. Ceroni, *Nanoscale*, 2020, **12**, 7921–7926.

3 R. Mazzaro, A. Gradone, S. Angeloni, G. Morselli, P. G. Cozzi, F. Romano, A. Vomiero and P. Ceroni, *ACS Photonics*, 2019, **6**, 2303–2311.

4 Y. Liu, C. Yu, H. Jin, B. Jiang, X. Zhu, Y. Zhou, Z. Lu and D. Yan, *J. Am. Chem. Soc.*, 2013, **135**, 4765–4770.

5 I. Coropceanu and M. G. Bawendi, *Nano Lett.*, 2014, **14**, 4097–4101.

6 S. K. Panigrahi and A. K. Mishra, *Photochem. Photobiol. Sci.*, 2019, **18**, 583–591.

7 K. Suzuki, A. Kobayashi, S. Kaneko, K. Takehira, T. Yoshihara, H. Ishida, Y. Shiina, S. Oishi and S. Tobita, *Phys. Chem. Chem. Phys.*, 2009, **11**, 9850–9860.

8 C. Würth, M. Grabolle, J. Pauli, M. Spieles and U. Resch-Genger, *Nat. Protoc.*, 2013, **8**, 1535–1550.

9 M. R. . Hessel, C. M.; Reid, D.; Panthani, M. G.; Rasch, B. A. Goodfellow, B. W.; Wei, J.; Fujii, H.; Akhavan, V.; Korgel, C. M. Hessel, D. Reid, M. G. Panthani, M. R. Rasch, B. W. Goodfellow, J. Wei, H. Fujii, V. Akhavan and B. A. Korgel, *Chem. Mater.*, 2012, **24**, 393–401.

10 M. Locritani, Y. Yu, G. Bergamini, M. Baroncini, J. K. J. K. Molloy, B. A. B. A. Korgel and P. Ceroni, *J. Phys. Chem. Lett.*, 2014, **5**, 3325–3329.

11 F. Serra and E. M. Terentjev, *Macromolecules*, 2008, **41**, 981–986.

12 K. S. Schanze, T. F. Mattox and D. G. Whitten, *J. Org. Chem.*, 1983, **48**, 2808–2813.

13 P. D. Wildes, J. G. Pacifici, G. Irick, D. G. Whitten, P. D. Wildes, J. G. Pacifici, G. Irick, D. G. Whitten, P. D. Wildes, J. G. Pacifici and G. Irick, *J. Am. Chem. Soc.*, 1971, **93**, 2004–2008.